



Soft X-ray detection and photon counting spectroscopy with commercial 4H-SiC Schottky photodiodes



S. Zhao*, T. Gohil, G. Lioliou, A.M. Barnett

Semiconductor Materials and Devices Laboratory, Department of Engineering and Design, School of Engineering and Informatics, University of Sussex, Falmer, Brighton BN1 9QT, UK

ARTICLE INFO

Article history:

Received 1 March 2016

Received in revised form

11 May 2016

Accepted 12 May 2016

Available online 13 May 2016

Keywords:

X-ray detector

Photodiode

Silicon carbide

COTS

Commercial off the shelf

ABSTRACT

The results of electrical characterisation and X-ray detection measurements of two different active area (0.06 mm² and 0.5 mm²) commercial 4H-SiC Schottky photodiodes at room temperature are reported. The devices exhibited low dark currents (less than 10 pA) even at a high electric field strengths (403 kV/cm for 0.06 mm² diodes; 227 kV/cm for 0.5 mm² diodes). The results of the X-ray measurements indicate that the diodes can be used as photon counting spectroscopic X-ray detectors with modest energy resolutions: FWHM at 5.9 keV of 1.8 keV and 3.3 keV, for the 0.06 mm² and 0.5 mm² devices, respectively. Noise analysis of the photodiodes coupled to a custom low noise charge sensitive preamplifier is also presented.

© 2016 The Authors. Published by Elsevier B.V. This is an open access article under the CC BY license (<http://creativecommons.org/licenses/by/4.0/>).

1. Introduction

Wide bandgap semiconductors such as AlGaAs [1,2], GaN [3,4], GaAs [5,6] and SiC [7–10], are good potential candidate materials for radiation detectors required to operate in harsh environments and as such have received significant attention in recent years. SiC has been subject to particularly intensive study [11,12]. The wide bandgap of SiC (4H-SiC=3.27 eV; 6H-SiC=2.86 eV), brings the benefits of a good visible–blind performance and low leakage currents even when operating at high temperature [9]. Furthermore, SiC detectors are radiation hard [13,14].

SiC has shown particular promise for use as an X-ray detector. The first experimental report of X-ray spectroscopy with SiC was in 2001; Np L X-rays and the 59.5 keV γ -ray emissions from an ²⁴¹Am radioisotope γ -ray source were detected using a heavily N-doped 4H-SiC device with a Schottky contact [15]. More recently, SiC detectors coupled to ultra-low-noise preamplifier electronics have been demonstrated to have excellent energy resolution (233 eV FWHM at 5.9 keV) even at high temperatures (100 °C) [10].

Whilst SiC UV photodiodes have been readily commercially available from standard electronic component retailers for some years, there has so far been no report of the potential utility of these readily available devices as X-ray detectors. If such relatively cheap and easily available devices can be used to detect X-rays, it

opens possibilities for low cost, radiation hard and high temperature tolerant X-ray detectors to be used for applications such as university-led cubesat missions and industrial applications.

In this paper, results are reported characterising four commercially available 4H-SiC UV photodiodes of two different active areas, as current mode and photon counting spectroscopic detectors of soft X-rays from a ⁵⁵Fe radioisotope X-ray source (Mn K α =5.9 keV; Mn K β =6.5 keV).

2. 4H-SiC UV photodiodes

Four SiC UV Schottky photodiodes of two different active areas (0.06 mm² and 0.5 mm²) manufactured by sglux SolGel Technologies GmbH, Berlin, Germany [16,17], were purchased from a standard electronics retailer. The photodiodes were supplied mounted in TO-18 packages. The UV windows of the TO-18 packages were removed as shown in Fig. 1 so that the devices could be directly illuminated with X-rays.

3. Experiments

3.1. Electrical characterisation

3.1.1. Capacitance–voltage measurements

The capacitances of all four photodiodes were measured as

* Corresponding author.

E-mail address: Shifan.Zhao@sussex.ac.uk (S. Zhao).

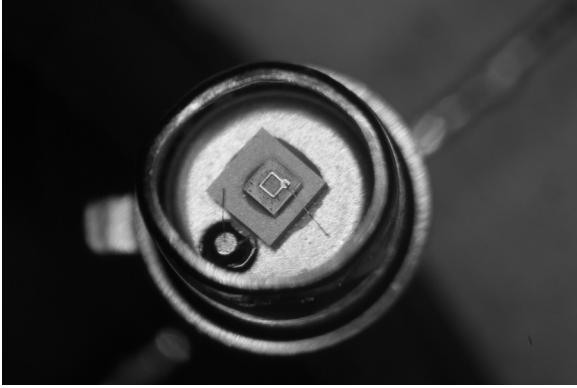


Fig. 1. Photograph of packaged 0.5 mm² SiC Schottky photodiode with UV window removed.

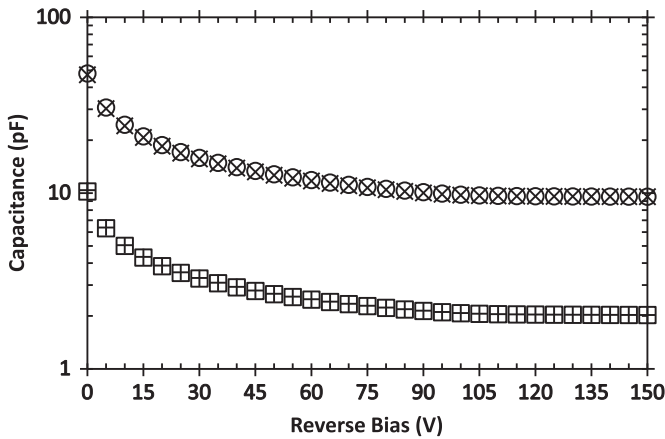


Fig. 2. Measured capacitances of two 0.06 mm² (+ symbols and open squares) and two 0.5 mm² (× symbols and open circles) photodiodes as functions of applied reverse bias.

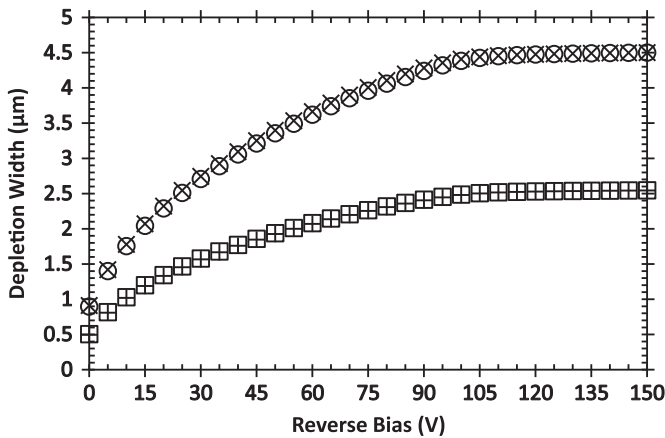


Fig. 3. Calculated depletion width of the 0.06 mm² (+ symbols and open squares) and 0.5 mm² (× symbols and open circles) photodiodes as a function of applied reverse bias.

functions of applied reverse bias at room temperature (24 °C) up to 150 V in 1 V steps using an HP 4275 A Multi Frequency LCR meter and a Keithley 6487 Picoammeter/Voltage Source as the external voltage supply. The AC test voltage signal magnitude and frequency of the LCR meter were set at 60 mV r.m.s. and 1 MHz, respectively. National Instruments Labview software was used to automate the capacitance measurements. In order to extract the capacitances of the photodiodes themselves, the bond wires of sacrificial devices of the same type were removed to measure

packaging capacitances. The capacitance of each photodiode was calculated by subtracting the capacitances of packages (0.67 pF for the 0.06 mm² photodiodes and 0.65 pF for 0.5 mm² photodiodes) from the total capacitances of the packaged devices. The measured capacitances and the calculated depletion width of each diode as functions of applied reverse bias are shown in Figs. 2 and 3, respectively. The photodiodes were fully depleted at an applied reverse bias of 120 V and 150 V for the 0.06 mm² and 0.5 mm² devices, respectively. The thickness of the depletion widths of the 0.06 mm² and 0.5 mm² photodiodes were determined to be 2.5 μm and 4.5 μm at 150 V reverse bias, respectively. In comparison to other previously reported wide bandgap X-ray detectors, they are thinner than previously reported GaAs X-ray detectors (7 μm) [5] and SiC X-ray detectors (25 μm) [10] but comparable to AlGaAs X-ray detectors (1.7 μm) [1].

Assuming the efficiency of these diodes is determined by the absorption in the depletion width, their efficiencies can be estimated from,

$$QE=1-e^{-\mu t} \quad (1)$$

where μ is the linear attenuation coefficient at the particular X-ray energy and t is the thickness of the depletion width. Fig. 4 shows the quantum efficiency for these photodiodes at their maximum depletion widths (150 V reverse bias) at X-ray energies up to 10 keV. The quantum efficiencies of the devices at 5.9 keV ($\mu_{5.9 \text{ keV}}=348 \text{ cm}^{-1}$; $\mu_{6.49 \text{ keV}}=263 \text{ cm}^{-1}$ [18]) were 0.085 and 0.145, for the 0.06 mm² and 0.5 mm² photodiodes, respectively.

3.1.2. Current-voltage measurements

The leakage currents of the four photodiodes were measured as functions of applied reverse bias from 0 V to 100 V at room temperature (24 °C) with 1 V per step using a Keithley 6487 Picoammeter/Voltage Source. The results are presented in Fig. 5. National Instruments Labview software was used to automate the measurements. The photodiodes have low leakage currents (less than 10 pA) at high reverse bias (corresponding to leakage current densities of 937 pA/cm² and 347 pA/cm² at electric fields of 403 kV/cm for the 0.06 mm² diodes; and 1.4 nA/cm² and 1.18 nA/cm² at electric fields of 227 kV/cm for the 0.5 mm² diodes). These are greater than some previously reported SiC X-ray detectors (1 pA/cm² with mean electric fields of 53 and 103 kV/cm at room temperature) [10], but better than semi-insulating SiC X-ray photodiodes (from 2.6 to 65 nA/cm² with internal electric fields from

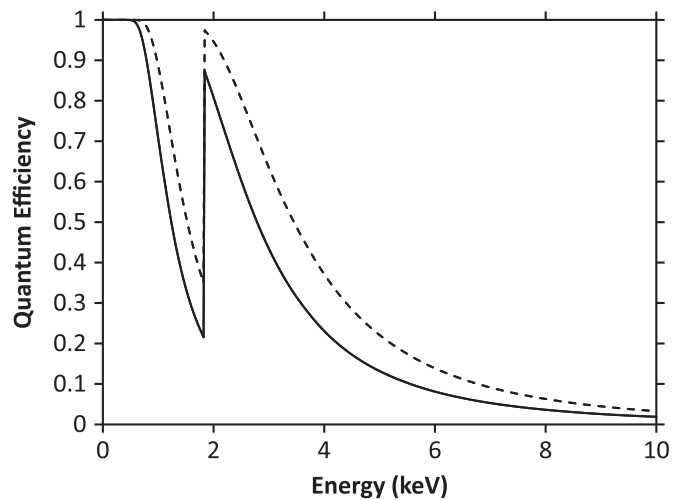


Fig. 4. The calculated quantum efficiencies of the SiC 0.06 mm² photodiodes – depletion layer thickness=2.5 μm (solid line), and 0.5 mm² photodiodes – depletion layer thickness=4.5 μm (dash line) at 150 V reverse bias with varying X-ray energy. The discontinuity at 1.8 keV is the Si K absorption edge.

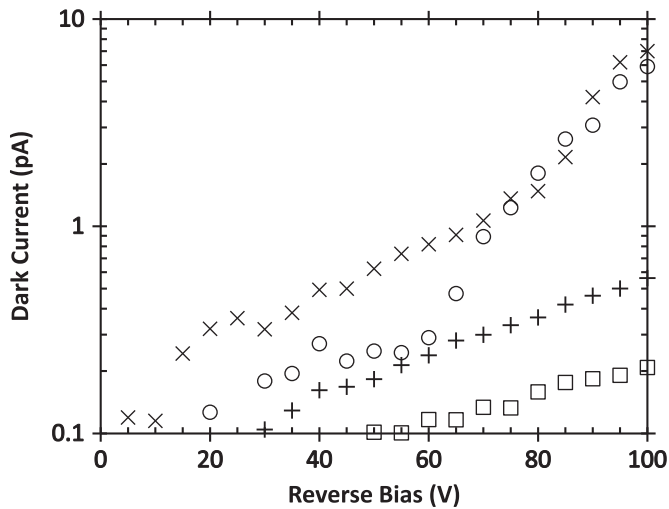


Fig. 5. Leakage current as a function of applied bias for the 0.06 mm² (+ symbols and open squares) and 0.5 mm² (x symbols and open circles) photodiodes.

7 to 28 kV/cm [8] and GaAs X-ray photodiodes (e.g. 17.4 nA/cm² with internal electric field 22 kV/cm) [5].

3.2. Current mode X-ray measurements

In order to characterize the response of the diodes to illumination with soft X-rays, an ⁵⁵Fe radioisotope X-ray source (Mn K α =5.9 keV; Mn K β =6.5 keV; activity=260 MBq; active area=28.27 mm²) was placed 2 mm above the diodes. The reverse bias was increased from 0 V to 100 V in 1 V steps. The measured photocurrent (the current measured with the devices illuminated with the previously measured leakage current subtracted) are presented for the 0.06 mm² and 0.5 mm² devices in Fig. 6.

Given the quantum efficiencies of the devices computed from the calculated depletion widths at 100 V reverse bias (2.48 μ m and 4.4 μ m, for the 0.06 mm² and 0.5 mm² devices, respectively), the activity geometry of the ⁵⁵Fe radioisotope X-ray source, and the relative emission probabilities (Mn K α 5.9 keV=0.245; Mn K β =6.49 keV=0.0338 [23]), the calculated expected photocurrents at 100 V reverse bias of 0.06 mm² photodiodes (0.44 pA) and 0.5 mm² photodiodes (6.3 pA), assuming only charge created in the depletion width contributed to the signal and 100% charge

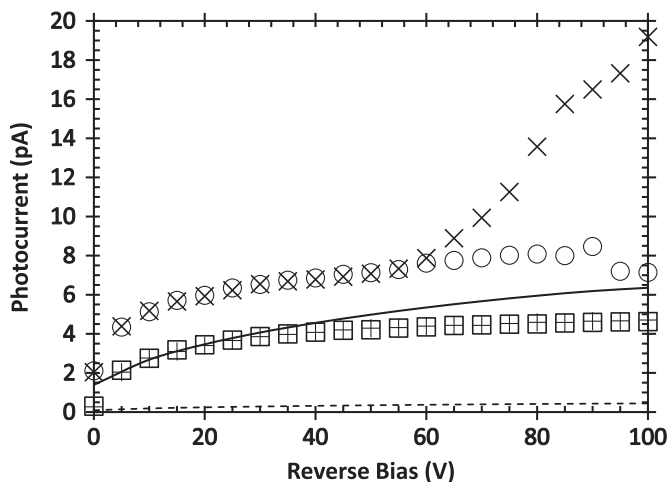


Fig. 6. Photocurrent as a function of applied reverse bias for the 0.06 mm² (+ symbols and open squares) and 0.5 mm² (x symbols and open circles) photodiodes. Expected photocurrent for the 0.06 mm² diodes (dash line) and 0.5 mm² (solid line).

collection efficiency [19], were much smaller than the measured photocurrents of the 0.06 mm² photodiodes (4.6 pA) and 0.5 mm² photodiodes (18 pA) at 100 V reverse bias. The greater than expected photocurrent suggests that there were significant contributions to the signal from charge created outside of the depletion region by photons absorbed there. Furthermore, one 0.5 mm² photodiode showed an exponential trend in photocurrent at reverse biases > 60 V indicative of avalanche multiplication even though the electric field strength, assuming a uniform electric field across the depletion layer, was lower than that at which significant impact ionization has been previously observed to occur [20]. This may have been due to defects in the material of the detector leading to localised regions of high electric field strength.

3.3. Photon counting X-ray spectroscopy

The diodes were each in turn connected to a custom-made low-noise charge-sensitive preamplifier with a 2N4416A silicon input JFET (capacitance=2 pF). An ORTEC 572 A shaping amplifier and a multi-channel analyser (MCA) were connected to the preamplifier. Spectra were accumulated using an ⁵⁵Fe radioisotope X-ray source. The ⁵⁵Fe radioisotope X-ray source was placed 2 mm above the diodes. Spectra were accumulated at reverse biases from 0 V to 100 V in 10 V steps. The temperature of the detector and preamplifier was 22 °C. The live time limit for each spectrum was 60 s.

Because of the large capacitances and low leakage currents of these devices, the longest shaping time available (10 μ s) was selected [21,22]. The resulting spectra were calibrated in energy terms by using the position of the zero energy noise peak and the position of the fitted Mn K α at 5.9 keV for each spectrum as points of known energy on MCA's charge scale and assuming a linear variation of detected charge with energy. The energy resolution of the devices as quantified by the full width half maximum (FWHM) of the 5.9 keV peak is presented in Fig. 8 as a function of applied reverse bias. A photopeak could not be resolved with the 0.5 mm² photodiodes at reverse biases below 50 V due to the large capacitance of the devices. For both sizes of device (0.06 mm² and 0.5 mm²) the best energy resolutions, 1.8 keV FWHM and 3.3 keV FWHM, were obtained at the maximum investigated reverse bias (100 V). The ⁵⁵Fe X-ray spectrum obtained at 100 V with one of the 0.06 mm² photodiodes is presented in Fig. 7; two Gaussians were fitted to the observed photopeak to represent the Mn K α (5.9 keV) and Mn K β (6.5 keV) emissions from the radioisotope X-ray source in the accepted ratio [23]. The MCA's low energy threshold was set at 2.85 keV as a compromise between minimising the number of noise counts from the tails of the zero energy noise peak and

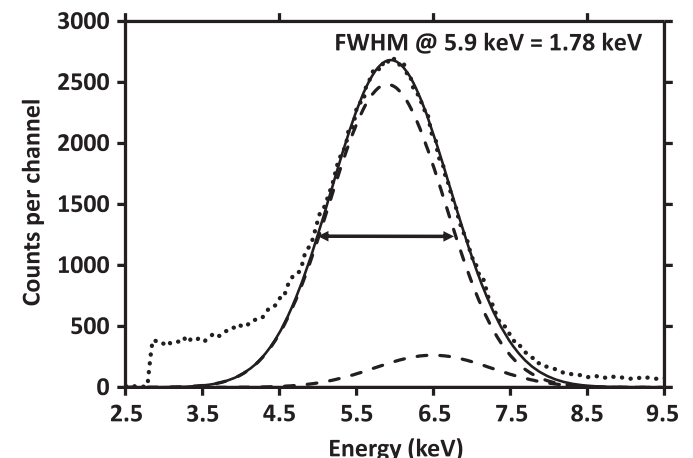


Fig. 7. ⁵⁵Fe X-ray spectrum obtained on one of the 0.06 mm² photodiodes at 100 V reverse bias. The dashed lines are the fitted Mn K α and K β peaks.

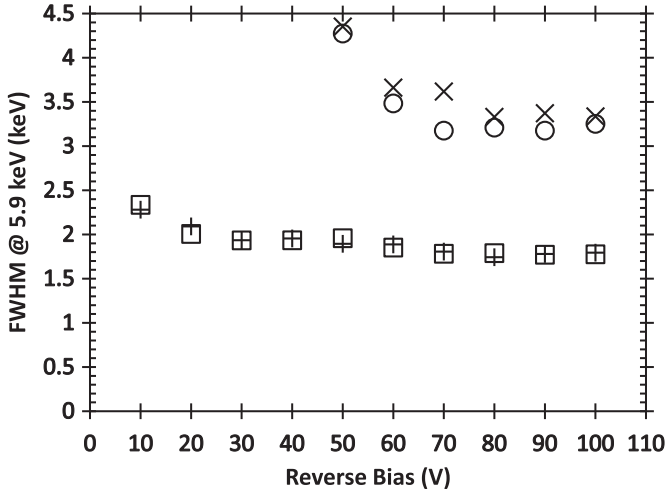


Fig. 8. Measured FWHM at 5.9 keV of 0.06 mm² (+ symbols and open squares) and 0.5 mm² (× symbols and open circles) photodiodes as functions of applied reverse bias.

maintaining the low energy response of the spectrometer. The energy resolutions at 5.9 keV were not as good as some wide bandgap devices specifically designed for X-ray detection e.g. GaAs mesa photodiodes (840 eV, area of 0.03 mm²; and 1.07 keV, area of 0.13 mm²) [24], AlGaAs X-ray detectors (1.1 keV, area of 0.03 mm² [25]; and 1.27 keV, area of 0.13 mm² [1]), and the best result of SiC X-ray detectors (196 eV at 30 °C, area of 0.4 mm²) [10]. However, the FWHM of the 0.06 mm² area diode was better than some larger area AlGaAs photodiodes (0.13 mm²) (1.95 keV) [26].

3.4. Noise analysis

The fundamental ‘Fano-limited’ energy resolution ($FWHM_{Fano}$) of a non-avalanche photodiode is given by,

$$FWHM_{Fano} = 2.355\omega\sqrt{FE/\omega} \quad (2)$$

where, ω is the average energy consumed in the generation an electron–hole pair (7.8 eV for SiC [27]), F is the Fano factor (0.1 for SiC [10]), and the E is the energy of the X-ray photon [28].

The energy resolution of a photodiode spectrometer is further influenced by noise from incomplete charge collection and electronic noise from the connection of the detector to the pre-amplifier, such that as the electronic noise arises not only from the shot noise of the detector but also the noise from the amplification system. Such that Eq. (2) becomes

$$FWHM = 2.355\omega\sqrt{\left(\frac{FE}{\omega}\right) + A^2 + R^2} \quad (3)$$

where, A and R are the equivalent noise charge contributions from electronic noise and incomplete charge collection, respectively [28]. The expected Fano limited energy resolution, $FWHM_{Fano}$ in SiC is 160 eV FWHM at 5.9 keV [10]. Therefore, it is essential to consider the other noise sources contributing to the measured energy resolution of the system.

The electronic noise of this system consists of five contributors: series white noise, parallel white noise, 1/f series noise, dielectric noise and the induced gate drain current noise [28]. A detailed explanation of the origin of each electronic contributors can be found in Ref. [1]. The total electronic noise contribution was measured for the system with the 0.06 mm² devices by injecting a delta test pulse signal into the preamplifier with the detector connected but unilluminated [21,22,29].

The dielectric noise (and series white noise from unknown

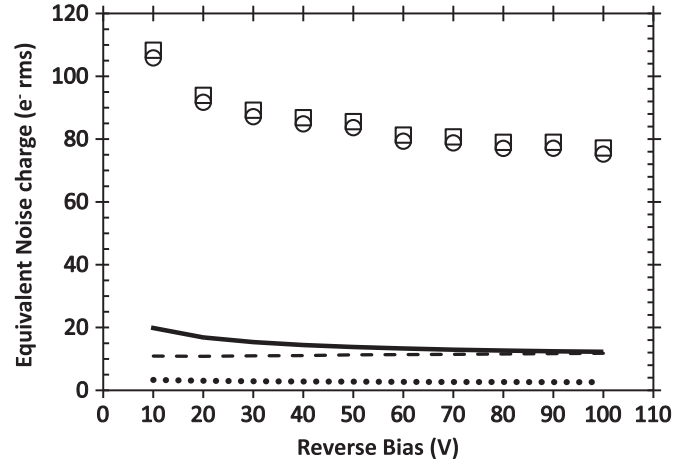


Fig. 9. Calculated electronic noise contributions for one 0.06 mm² photodiode, connected to the custom low-noise charge-sensitive preamplifier, at varied reverse bias. Measured electronic noise (open squares), computed dielectric noise and series white noise from unknown stray capacitances (open circles), white series noise (square dot line), white parallel noise (dash line) and 1/f series noise (round dot line).

stray capacitances [1]) can be calculated by the subtraction of the calculated series white noise including induced gate drain current noise, parallel white noise, and 1/f noise in quadrature from the measured total electronic noise [5]. The other noise components were calculated as per Ref. [1]. The calculated electronic noise components are presented as a function of reverse bias in Fig. 9. As is the case for other detectors connected to similar charge-sensitive preamplifiers, the dielectric noise (and noise from stray capacitances) is the most significant noise component [1,5]. Such noise is thought to arise from dielectric materials of the capacitances and packages [21]. The presently reported preamplifier used a wire-end input JFET for convenience; a bare die JFET directly wire-bonded to the detector would be expected to significantly reduce the noise. If this noise could be eliminated entirely, an energy resolution (FWHM at 5.9 keV) of 1.1 keV could be achieved with the 0.06 mm² photodiode.

Incomplete charge collection noise is related to the detector’s charge diffusion and collection properties as well as to the trap density distribution in the detector [28]. In this system, the incomplete charge collection noise can be calculated by subtracting in quadrature the predicted Fano noise and the total electronic noise from the measured energy resolution at 5.9 keV. The calculated contributions from incomplete charge collection for the 0.06 mm² photodiode are shown in Fig. 10. Interestingly, the incomplete charge collection noise was independent of applied electric field. This supports the hypothesis – introduced in Section 3.2 to explain the greater than expected photocurrent – that significant amounts of charge created outside of the depletion region (by photons absorbed in those positions) contributed to the detected signal. Since the applied bias mainly resulted in an electric field across the epi-layer/depletion region, the field strength in the volume below the depletion region remained low, regardless of applied bias. Thus the incomplete charge collection noise, which probably arose from recombination of electrons and holes in the low field region remained constant. The data and explanation are consistent high quality material close to top Schottky contact exhibiting comparatively little charge trapping and a volume of material with consistently low electric field strength below it showing moderate amounts (≈ 58 e⁻ rms equivalent noise charge) of incomplete charge collection noise.

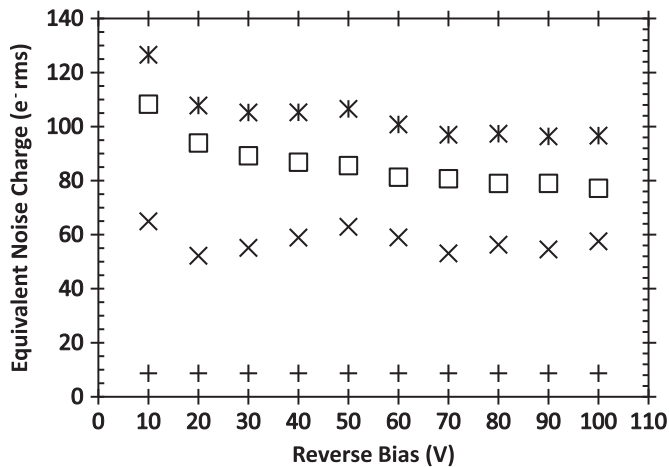


Fig. 10. Computed noise contributions of one of the 0.06 mm² photodiodes at varied reverse bias. Total FWHM measured at 5.9 keV (stars), electronic noise (open squares), incomplete charge collection noise (× symbols), and the Fano noise (+ symbols).

4. Conclusions and future work

Measurements characterizing four commercial 4H-SiC Schottky photodiodes of two different areas (0.06 mm² and 0.5 mm²) at room temperature have been presented. The measurements of capacitance as functions of applied reverse bias showed consistent characteristics between photodiodes of the same active area. The depletion widths (2.5 μm and 4.5 μm, respectively) of the devices were calculated based on the capacitance measurements. The diodes were found to be fully depleted at ≥ 120 V reverse bias. Measurements of leakage current as a function of applied reverse bias showed low leakage currents among these diodes (less than 10 pA) at 100 V reverse bias; the current densities were found between 300 and 900 pA/cm² with the 0.06 mm² diodes (at electric field strengths of 403 kV/cm) and 1.2 to 1.4 nA/cm² with 0.5 mm² diodes (at electric field strengths of 227 kV/cm).

The performance of these devices as X-ray detectors was investigated by the measuring the photocurrent generated when the devices were illuminated by an ⁵⁵Fe radioisotope X-ray source, and by connecting the photodiodes to a custom low-noise charge-sensitive preamplifier and investigating their performance as detectors for photon counting X-ray spectroscopy. The photocurrents were measured to be 5 pA with the 0.06 mm² photodiodes and 7–19 pA with 0.5 mm² devices. The detectors functioned as photon counting spectroscopic X-rays detectors with modest energy resolution (the FWHM at 5.9 keV of the 0.06 mm² and 0.5 mm² diodes were 1.8 keV and 3.3 keV at 100 V reverse bias, respectively). Although the energy resolutions were not as good as many custom X-ray detectors, the results indicated these photodiodes can be used for photon counting X-ray spectroscopy at room temperature albeit with modest energy resolution. Noise analysis of this system was also presented. It showed that dielectric noise and series white noise from stray capacitances were the dominant noise sources in the system. If the noise, which was a consequence of the non-optimal design of the connection of the detectors to the preamplifier, could be entirely eliminated the energy resolution would be expected to improve to 1.1 keV.

In future publications, the performance of these devices at high temperature will be reported, as will characterisation of the detectors when illuminated with X-ray photons of different energies.

Acknowledgements

This work was in part supported by the Science and Technologies Facilities Council, United Kingdom, through grants ST/M002772/1 and ST/M004635/1 (University of Sussex, A.M.B., PI). The authors acknowledge funding received from The Royal Society, UK for RG130515 (University of Sussex, A.M.B., PI). T.G. acknowledges funding received in the form of a Ph.D. studentship from the Engineering and Physical Sciences Research Council, UK, and the University of Sussex, UK. G.L. acknowledges funding received from the University of Sussex, UK, in the form of a Ph.D. scholarship.

Authors' Data Statement: Data underlying this work are subject to commercial confidentiality. The Authors regret that they cannot grant public requests for further access to any data produced during the study.

References

- [1] A.M. Barnett, G. Ljoliou, J.S. Ng, Nucl. Instrum. Methods A 774 (2015) 29.
- [2] J. Lauter, D. Protić, A. Förster, H. Lüth, Nucl. Instrum. Methods A 356 (1995) 324.
- [3] A. Owens, A. Barnes, R.A. Farley, M. Germain, P.J. Sellin, Nucl. Instrum. Methods A 695 (2012) 303.
- [4] A. Motogaito, H. Watanabe, K. Hiramatsu, K. Fukui, Y. Hamamura, K. Tadamoto, Phys. Status Solidi A 200 (2003) 147.
- [5] G. Ljoliou, X. Meng, J.S. Ng, A.M. Barnett, Nucl. Instrum. Methods A 813 (2016) 1.
- [6] A. Owens, M. Bavdaz, A. Peacock, A. Poelaert, H. Andersson, S. Nenonen, H. Sipilä, L. Tröger, G. Bertuccio, Nucl. Instrum. Methods A 466 (2001) 168.
- [7] J. Lees, A.M. Barnett, D. Bassford, R. Stevens, A. Horsfall, J. Instrum. 6 (2011) C011032.
- [8] G. Bertuccio, D. Puglisi, A. Pullia, C. Lanzieri, IEEE Trans. Nucl. Sci. 60 (2013) 1436.
- [9] N. Watanabe, T. Kimoto, J. Suda, Appl. Phys. Express. 5 (2012) 094101.
- [10] G. Bertuccio, S. Caccia, D. Puglisi, D. Macera, Nucl. Instrum. Methods A 652 (2011) 193.
- [11] M.V.S. Chandrashekar, C.I. Thomas, H. Li, M.G. Spencer, A. Lal, Appl. Phys. Lett. 88 (2006) 033506.
- [12] X. Chen, H. Zhu, J. Cai, Z. Wu, J. Appl. Phys. 102 (2007) 024505.
- [13] F. Nava, G. Bertuccio, A. Cavallini, E. Vittone, Meas. Sci. Technol. 19 (2008) 102001.
- [14] K.C. Mandal, P.G. Muzykov, S.K. Chaudhuri, J.R. Terry, IEEE Trans. Nucl. Sci. 60 (2013) 2888.
- [15] G. Bertuccio, R. Casiraghi, F. Nava, IEEE Trans. Nucl. Sci. 48 (2001) 232.
- [16] Anon, Broadband SiC based UV photodiode A=0.06 mm², SG015–18, Rev.6.0, SGLux SolGel Technologies GmbH, Berlin, Germany, N.D.
- [17] Anon, Broadband SiC based UV photodiode A=0.50 mm², SG01D–18, Rev.6.0, SGLux SolGel Technologies GmbH, Berlin, Germany, N.D.
- [18] D.T. Cromer, D. Liberman, J. Chem. Phys. 53 (1970) 1891.
- [19] S.M. Sze, Semiconductor Devices, Physics and Technology, Wiley, New York, 1985.
- [20] S. Loh, B. Ng, J. David, S. Soloviev, H. Cha, IEEE Trans. Electron Dev. 55 (2008) 1984.
- [21] G. Bertuccio, A. Pullia, G. De Geronimo, Nucl. Instrum. Methods A 380 (1996) 301.
- [22] A.M. Barnett, J.E. Lees, D.J. Bassford, J.S. Ng, Nucl. Instrum. Methods A 673 (2012) 10.
- [23] U. Schötzgig, Appl. Radiat. Isot. 53 (2000) 469.
- [24] A.M. Barnett, Nucl. Instrum. Methods A 756 (2014) 39.
- [25] A.M. Barnett, D.J. Bassford, J.E. Lees, J.S. Ng, C.H. Tan, J.P.R. David, Nucl. Instrum. Methods A 621 (2010) 453.
- [26] A.M. Barnett, J.E. Lees, D.J. Bassford, J. Instrum. 8 (2013) P10014.
- [27] G. Bertuccio, R. Casiraghi, IEEE Trans. Nucl. Sci. 50 (1) (2003) 175.
- [28] A. Owens, Compound Semiconductor Radiation Detectors, CRC Press, Boca Raton, 2012.
- [29] American National standards Institute, An American National Standard IEEE Standard Test Procedures for Amplifiers and Preamplifiers for Semiconductor Radiation Detectors for Ionizing Radiation, in: Proceedings of IEEE Standard Test Procedures for Amplifiers and Preamplifiers for Semiconductor Radiation Detectors. Measurement. <http://dx.doi.org/10.1109/IEEESTD.1976.120672>.